Spherical probe in a flowing plasma

1971 J. Phys. A: Gen. Phys. 4 142

(http://iopscience.iop.org/0022-3689/4/1/017)

J. Phys. A: Gen. Phys., 1971, Vol. 4. Printed in Great Britain

Spherical probe in a flowing plasma

J. G. ANDREWS and D. T. SWIFT-HOOK
Marchwood Engineering Laboratories, Central Electricity Generating Board, Marchwood, Southampton, England
MS. received 25th August 1970

Abstract. Ion flow is important in many laboratory discharges, vacuum switches, gas-filled valves, thyratrons and space satellites. A model is presented for subsonic ion flow past a negative spherical probe immersed in a collisionless ionization-free plasma; a stagnation point develops downstream. Although the floating potential given by previous analyses (which all assume spherical symmetry) is substantially correct, there is some dependence on the ion flow velocity (a few % at $M = 0{\cdot}5$). Thus the change in floating potential can be used to measure ion flow. In general, only slight modification needs to be made to low pressure probe theories in order to include flow effects.

1. Introduction

In recent years the 'cold ion approximation' has been applied to a wide variety of problems in low pressure plasmas. In the cold ion approximation the velocity dispersion of the ions is ignored, that is, all the ions are assumed to have the same velocity at any point in the plasma. This model has been used to describe waves in plasmas (Woods 1965, Bertotti *et al.* 1966, Allen and Andrews 1970, Rosa and Allen 1970, Andrews 1970), plasmas in magnetic fields (Forrest and Franklin 1966) and the problem of the transition from a collisionless to a diffusion-dominated positive column (Forrest and Franklin 1968). There has also been some interest in using the cold ion approximation to describe asymmetrical ion flow in a plasma; Stangeby and Allen (1970) have used it to show that the plasma boundary must coincide with a Mach surface, that is, the normal component of the ion velocity at the plasma boundary is equal to the ion speed of sound c given by

$$c = (kT_e/m_i)^{1/2} \tag{1}$$

where k is Boltzmann's constant, T_e is the electron temperature and m_i is the ion mass. Andrews and Stangeby (1970) have pointed out that this result still holds even when ionization and collisions are taken into account.

In the present paper we consider a spherical probe immersed in a collisionless ionization-free plasma with a superimposed ion drift. The theory of a spherical probe in a collisionless plasma with no asymmetry in the ion flow is well documented (Mott-Smith and Langmuir 1926, Bohm *et al.* 1949, Allen *et al.* 1957, Bernstein and Rabinowitz 1959, Lam 1965, Bienkowski and Chang 1968). However, in most situations of practical interest (including many laboratory discharges, vacuum switches, gas-filled valves, thyratrons and space-satellites) asymmetrical ion flow exists. This means that existing probe theories are in doubt. At high pressures, for example, Thomas (1969) and Clements and Smy (1969) have shown that flow effects can produce two orders of magnitude difference in probe currents from those measured with no flow (Su and Lam 1963). We shall investigate flow effects at low pressures to see how low pressure probe theories need to be modified.

2. The general approach

Consider a plasma with ion flow but no collisions or ionization. The ion motions follow the steady state continuity and momentum equations (see for example Woods 1965)

$$\nabla . (n\boldsymbol{v}) = 0 \tag{2}$$

$$\nabla . (n\boldsymbol{v}\boldsymbol{v}) = -(ne/m_i)\nabla V \tag{3}$$

where n is the ion number density, $\boldsymbol{v}$ is the ion drift velocity, e is the ionic charge and V is the electrostatic potential. The plasma is assumed to be quasi-neutral. The probe voltage is sufficiently negative that the electron current drawn by the probe is negligible compared with random electron current in the plasma; then we can take (Mott-Smith and Langmuir 1926) the electrons to have a Boltzmann density distribution

$$n = n_0 \exp(eV/kT_e) \tag{4}$$

where n_0 is the number density in the undisturbed plasma. For convenience, we shall only consider plasmas in which the ion flow is irrotational, so that

$$\nabla \times \boldsymbol{v} = 0. \tag{5}$$

Eliminating n and V from equations (2)–(5) yields

$$c^2 \nabla . \boldsymbol{v} = \tfrac{1}{2}(\boldsymbol{v} . \nabla) v^2. \tag{6}$$

Thus, the problem of steady collisionless ion flow in an ionization-free plasma reduces to that of solving a first-order nonlinear partial differential equation in the ion velocity subject to various prescribed boundary conditions. Let us call this equation (6) the *general ion flow equation.*

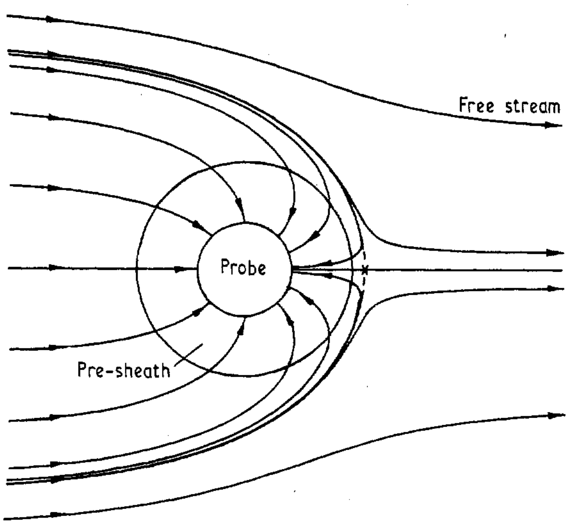

Figure 1. Ion trajectories around the probe for $M = 0{\cdot}1$.

As an example consider collisionless ion flow past a spherical probe which is biased negatively with respect to the plasma (see figures 1 and 2). In order to simplify the analysis, we ignore the effect of the supporting rod and take the ions to be unidirectional at infinity (which makes $\nabla \times \boldsymbol{v}$ vanish identically everywhere) with a velocity

U such that $U^2/c^2 \ll 1$, that is, the ion flow is substantially subsonic. If the ions are far enough away from the probe then the probe field is very weak, so that $v^2/c^2 \ll 1$ and compressibility effects are negligible. Let us call this region the *free stream*. This situation is quite different for the ions in the plasma close to the probe (the *pre-sheath*

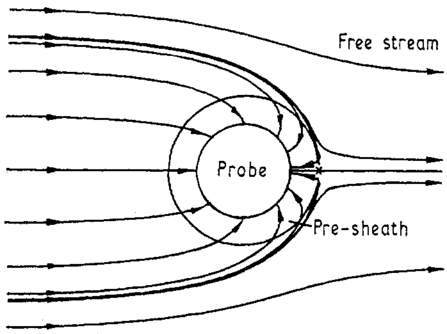

Figure 2. Ion trajectories around the probe for $M = 0{\cdot}3$.

region). According to the theory of a spherical probe collecting a radially symmetric ion flow (Bohm *et al.* 1949) we know that $v^2/c^2 \to 1$ at the plasma boundary surrounding the probe. We can similarly expect v^2/c^2 to be of order unity near the probe in our case with asymmetrical ion flow. Hence, compressibility effects in the pre-sheath region *are* significant; they can be dealt with approximately by taking linear perturbations of the radially-symmetric solution. In the absence of flow the region containing the pre-sheath extends out to infinity.

The general approach in this paper will be to find approximate solutions to the general ion flow equation (6) that are valid in the free stream and in the pre-sheath region respectively, and then to join the two solutions together at some appropriate boundary.

3. The free stream

At a sufficient distance from the probe the influence of the electric field is very weak and $v^2/c^2 \ll 1$. In this region of the flow (the free stream) equation (6) reduces to

$$\nabla . \boldsymbol{v} \simeq 0.$$

Defining a velocity potential ϕ_1 (where subscript 1 refers to the free stream), we have approximately that

$$\nabla^2\phi_1 = 0. \tag{7}$$

The ion velocity in the free stream is $\boldsymbol{v}_1 = -\nabla\phi_1$. Equation (7) is Laplace's equation. Using spherical polar coordinates (r, θ, ψ) with the z axis parallel to the ion flow at infinity and assuming azimuthal symmetry (with $\partial/\partial\psi \equiv 0$), those solutions which are finite on the axis of symmetry take the form

$$\phi_1 = \sum_{m=0}^{\infty} (A_m r^m + B_m r^{-m-1}) \mathrm{P}_m(\mu)$$

where $\mu = \cos\theta$ and $\mathrm{P}_m(\mu)$ is the Legendre polynomial of integral order m (see for example, Sneddon 1956). At large distances from the probe we require $v_{1r} \to U\cos\theta$, so that $A_m = 0$ for $m \neq 1$. Hence

$$\phi_1 = -UrP_1(\mu) + \sum_{m=0}^{\infty} B_m r^{-m-1} P_m(\mu). \tag{8}$$

The B_m are obtained when we match the above solution to that describing the pre-sheath at some appropriate boundary.

4. The pre-sheath

In the pre-sheath, close to the probe, the ion flow is substantially radially symmetric. For a first approximation $\partial/\partial\theta \equiv 0$ and the general ion flow equation (6) yields

$$\frac{c^2}{r^2}\frac{d(r^2 v_0)}{dr} = v_0^2 \frac{dv_0}{dr}$$

or

$$\frac{dv_0}{dr} = -\frac{2v_0}{r(1-v_0^2/c^2)}. \tag{9}$$

Note that $dv_0/dr \to \infty$ as $v_0 \to -c$, that is, the plasma solution breaks down (and a sheath develops) as the ions approach the speed of sound. If the sheath thickness is negligible compared with the probe radius a we can take the plasma boundary to be effectively at $r = a$ on the plasma scale, and equation (9) can be integrated analytically to give the radially symmetric velocity profile as

$$\frac{r^2}{a^2} = \left(-\frac{c}{v_0}\right) \exp\left\{-\tfrac{1}{2}\left(1 - \frac{v_0^2}{c^2}\right)\right\}. \tag{10}$$

Figure 3 shows this variation of v_0/c with r/a.

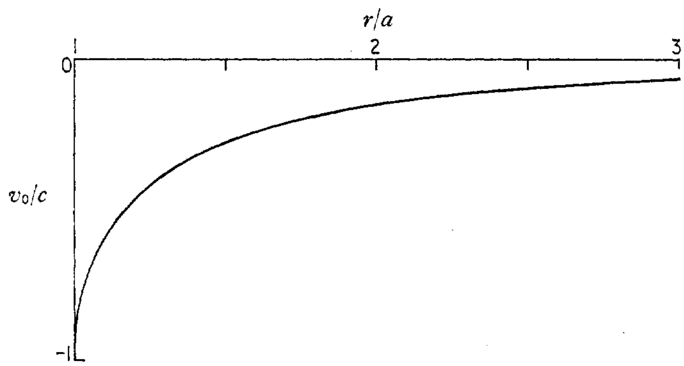

Figure 3. The radially symmetric velocity profile.

For a better approximation, we must allow for the effect of the asymmetry to the ion flow in the pre-sheath. Let

$$\boldsymbol{v}_2 = \boldsymbol{v}_0(r) + \boldsymbol{v}^*(r, \theta)$$

where the subscript 2 refers to the pre-sheath and the asterisk to the perturbed part of the solution. Substituting for $\boldsymbol{v}_2$ from the above equation into the general ion flow equation (6) and expanding in terms of the velocity components ,we have

$$c^2\left(\frac{1}{r^2}\frac{\partial(r^2 v_r^*)}{\partial r}+\frac{1}{r\sin\theta}\frac{\partial(\sin\theta\, v_\theta^*)}{\partial\theta}\right) = 2v_r^* v_0\left(\frac{\mathrm{d}v_0}{\mathrm{d}r}\right)+v_0^2\left(\frac{\partial v_r^*}{\partial r}\right)+N \qquad (11)$$

where

$$N = v_r^{*2}\frac{\mathrm{d}v_0}{\mathrm{d}r}+v_r^*(2v_0+v_r^*)\frac{\partial v_r^*}{\partial r}+2v_\theta^*(v_0+v_r^*)\frac{\partial v_\theta^*}{\partial r}$$
$$+v_\theta^{*2}\left(\frac{v_0+v_r^*}{r}+\frac{1}{r}\frac{\partial v_\theta^*}{\partial\theta}\right)$$

is nonlinear in v_r^* and v_θ^*. Let us solve equation (11) in the cases where the nonlinear terms can be neglected. This is so when $v^{*2} \ll c^2$, and the accuracy required can be judged from the condition $U^2 \ll c^2$ which we have already used in the free-stream. Provided v^* is $O(U)$ our approximation will be consistent. Examination of equations (42) and (43) together with (28) shows that this is indeed the case.

Neglecting N, equation (11) approximates to

$$c^2\left(\frac{1}{r^2}\frac{\partial(r^2 v_r^*)}{\partial r}+\frac{1}{r\sin\theta}\frac{\partial(\sin\theta\, v_\theta^*)}{\partial\theta}\right) = 2v_r^* v_0\frac{\mathrm{d}v_0}{\mathrm{d}r}+v_0^2\frac{\partial v_r^*}{\partial r}. \qquad (12)$$

Defining a perturbed velocity potential ϕ^*, we have $v_r^* = -\partial\phi^*/\partial r$ and $v_\theta^* = -r^{-1}\partial\phi^*/\partial\theta$, and equation (12) becomes

$$f(r)\frac{\partial^2\phi^*}{\partial r^2}+g(r)\frac{\partial\phi^*}{\partial r}+\frac{1}{(\sin\theta)}\frac{\partial(\sin\theta\,\partial\phi^*/\partial\theta)}{\partial\theta} = 0 \qquad (13)$$

where

$$f(r) = r^2(1-v_0^2/c^2)$$

and

$$g(r) = 2r\left(1-\frac{rv_0}{c^2}\frac{\mathrm{d}v_0}{\mathrm{d}r}\right).$$

Whereas equations (6) and (11) are highly nonlinear first-order equations, equation (13) is a linear second-order partial differential equation in ϕ^*. We can look for separable solutions of the form

$$\phi^* = R(r)\,T(\theta)$$

where R is a function of r only and T is a function of θ only. Then

$$\frac{1}{R}\left(f\frac{\mathrm{d}^2R}{\mathrm{d}r^2}+g\frac{\mathrm{d}R}{\mathrm{d}r}\right) = -\frac{1}{(T\sin\theta)}\frac{\mathrm{d}\{\sin\theta(\mathrm{d}T/\mathrm{d}\theta)\}}{\mathrm{d}\theta}.$$

The left-hand side cannot involve θ and the right-hand side cannot involve r, so both sides must be equal to a constant, which we shall write as $m(m+1)$ for convenience (and without loss of generality). We now have two equations

$$f\frac{\mathrm{d}^2R}{\mathrm{d}r^2}+g\frac{\mathrm{d}R}{\mathrm{d}r}-m(m+1)R = 0 \qquad (14)$$

$$\frac{\mathrm{d}\{\sin\theta(\mathrm{d}T/\mathrm{d}\theta)\}}{\mathrm{d}\theta}+m(m+1)T\sin\theta = 0. \qquad (15)$$

The solution of equation (14) is

$$R = R_m(r), \text{ say}$$

which we shall determine after matching the solution in the pre-sheath to the solution in the free stream on some suitable boundary. Equation (15) reduces to Legendre's equation of order m:

$$\frac{\mathrm{d}\{(1-\mu^2)\mathrm{d}T/\mathrm{d}\mu\}}{\mathrm{d}\mu}+m(m+1)T = 0$$

when we put $\mu = \cos\theta$. As in the case of the free stream (see § 3) we are only interested in the solution which is finite on the axis of symmetry,

$$T = C_m \mathrm{P}_m(\mu)$$

where C_m is a constant and P_m is the Legendre function or polynomial of order m. The complete solution of equation (13) for the linearized asymmetric perturbation can be expressed as the sum over integral values of m,

$$\phi^* = \sum_{m=1}^{\infty} C_m R_m(r)\mathrm{P}_m(\mu).$$

The total velocity potential in the pre-sheath including the symmetric solution becomes

$$\phi_2 = \phi_0(r)+\sum_{m=1}^{\infty} C_m R_m(r)\mathrm{P}_m(\mu) \tag{16}$$

where $\phi_0(r)$ is the radially symmetric velocity potential such that $v_0 = -\mathrm{d}\phi_0/\mathrm{d}r$. The C_m are obtained when we match the above solution to that for the free stream given in § 3.

5. Matching the free stream and the pre-sheath solutions

Our solution for the velocity potential in the free stream ϕ_1, given by equation (8), is reasonably accurate provided that $v^2/c^2 \ll 1$. Since v^2 approaches c^2 near the probe, there is clearly a limit to the extent to which we can apply this solution. Similarly, in the pre-sheath region, ϕ_2, given by equation (16), is accurate near the probe but not at a great distance from it. Let us introduce an artificial surface surrounding the probe where we shall attempt to match the free stream and the pre-sheath solutions.

Clearly, the components of the velocity must be continuous, so that

$$\frac{\partial\phi_1}{\partial r} = \frac{\partial\phi_2}{\partial r}$$

and

$$\frac{\partial\phi_1}{\partial\mu} = \frac{\partial\phi_2}{\partial\mu}.$$

Taking the surface to be the sphere $r = s$, say, equations (8) and (16) give

$$-U\mathrm{P}_1-\sum_{m=0}^{\infty} B_m(m+1)s^{-m-2}\mathrm{P}_m = -v_0(s)+\sum_{m=0}^{\infty} C_m R_m'(s)\mathrm{P}_m \tag{17}$$

and

$$-Us\mathrm{P}_1{}'+\sum_{m=1}^{\infty} B_m s^{-m-1}\mathrm{P}_m{}' = \sum_{m=1}^{\infty} C_m R_m(s)\,\mathrm{P}_m{}' \tag{18}$$

where

$$R_m{}' = \mathrm{d}R_m/\mathrm{d}s.$$

Using the recurrence relation

$$\mathrm{P}_{m+1}{}'(\mu)-\mu\mathrm{P}_m{}'(\mu) = (m+1)\mathrm{P}_m(\mu) \tag{19}$$

in equation (18) and equating coefficients (since the P_m are an orthogonal set of functions), we have

$$-B_0 s^{-2} = -v_0(s) \tag{20}$$

$$-U-2B_1 s^{-3} = C_1 R_1{}'(s), \qquad \text{for } m = 1 \tag{21}$$

$$-B_m(m+1)s^{-m-2} = C_m R_m{}'(s), \qquad \text{for } m > 1 \tag{22}$$

from equation (17), and

$$-Us+B_1 s^{-2} = C_1 R_1(s), \qquad \text{for } m = 1 \tag{23}$$

$$B_m s^{-m-1} = C_m R_m(s), \qquad \text{for } m > 1 \tag{24}$$

from equation (18) (the $m = 0$ terms vanish identically).

From equations (22) and (24), we can see that either B_m and C_m are always zero for $m > 1$, or

$$\frac{m+1}{s} = \frac{R_m{}'(s)}{R_m(s)}. \tag{25}$$

In fact it can be shown numerically that

$$\frac{R_m{}'(s)}{R_m(s)} > 0$$

but it is sufficient for our present purposes to note that $R_m(s)$ is a well-defined function, being a solution of equation (14). Equation (25) is not therefore in general satisfied so that

$$B_m = C_m = 0, \quad \text{for } m > 1. \tag{26}$$

From equations (21) and (23), we obtain

$$B_1 = -Us^3\frac{(1-\alpha)}{(2+\alpha)} \tag{27}$$

and

$$C_1 = -\frac{3Us}{R_1(s)(2+\alpha)} \tag{28}$$

where

$$\alpha = \frac{sR_1{}'(s)}{R_1(s)}. \tag{29}$$

Also, from equation (20) we have

$$B_0 = s^2 v_0(s). \tag{30}$$

The complete solutions for the velocity potentials in the free stream and the presheath then become

$$\phi_1 = \frac{B_0}{r}+\left(\frac{B_1}{r^2}-Ur\right)\cos\theta \tag{31}$$

and

$$\phi_2 = \phi_0(r) + C_1 R_1(r)\cos\theta \tag{32}$$

respectively.

It only remains to evaluate R_1. (Fortunately the higher order R_m have disappeared!).

Equation (14) gives

$$\left(1-\frac{v_0^2}{c^2}\right)\frac{\mathrm{d}^2R_1}{\mathrm{d}r^2}+\frac{2}{r}\left(1-\frac{rv_0}{c^2}\frac{\mathrm{d}v_0}{\mathrm{d}r}\right)\frac{\mathrm{d}R_1}{\mathrm{d}r}-\frac{2R_1}{r^2}=0. \tag{33}$$

This equation can be integrated analytically. It is, in fact, an exact differential

$$\frac{\mathrm{d}}{\mathrm{d}r}\left\{\left(1-\frac{v_0^2}{c^2}\right)\frac{\mathrm{d}R_1}{\mathrm{d}r}+\frac{2R_1}{r}\right\}=0.$$

Integrating, setting $R_1 = R_a$ and $\mathrm{d}R_1/\mathrm{d}r = 0$ at the plasma boundary $r = a$ (otherwise the second term in equation (33) would blow-up), we have

$$\left(1-\frac{v_0^2}{c^2}\right)\frac{\mathrm{d}R_1}{\mathrm{d}r}+\frac{2R_1}{r}=\frac{2R_a}{a}. \tag{34}$$

Dividing throughout by $v_0(1-v_0^2/c^2)$ and using equation (9), we obtain

$$\frac{1}{v_0}\frac{\mathrm{d}R_1}{\mathrm{d}v_0}-\frac{R_1}{v_0^2}=-\frac{rR_a}{av_0^2}$$

or

$$\frac{\mathrm{d}(R_1/v_0)}{\mathrm{d}v_0}=-\frac{rR_a}{av_0^2}.$$

Integrating again, using equation (10), gives

$$R_1 = R_a\left(-\frac{v_0}{c}\right)\{1+F(r)\} \tag{35}$$

where

$$F(r)=\int_{-v_0/c}^{1} y^{-5/2}\exp\{-\tfrac{1}{4}(1-y^2)\}\,\mathrm{d}y$$

and this completes the solution.

Equation (29) becomes

$$\alpha = \left(\frac{2}{1-v_0^2(s)/c^2}\right)\left(\frac{-sc/av_0(s)}{1+F(s)}-1\right) \tag{36}$$

using equations (34) and (35), and the full solution is given by equations (31) and (32) together with equations (27), (28), (30) and (35).

6. Velocity, potential and density profiles

We are now in a position to calculate the various physical quantities associated with the plasma flow. Consider first the free stream region. The ion velocity components are obtained by differentiating ϕ_1, given by equation (31), that is,

$$\begin{aligned} v_{1r} &= -\partial\phi_1/\partial r \\ &= \frac{B_0}{r^2}+\left(\frac{2B_1}{r^3}+U\right)\cos\theta \end{aligned} \tag{37}$$

and

$$v_{1\theta} = -\frac{1}{r}\frac{\partial\phi_1}{\partial\theta}$$

$$= \left(\frac{B_1}{r^3} - U\right)\sin\theta. \tag{38}$$

The total ion velocity is simply

$$v_1 = (v_{1r}^2 + v_{1\theta}^2)^{1/2}. \tag{39}$$

The electrostatic potential is obtained by applying energy conservation:

$$V_1 = -\tfrac{1}{2}m_i(v_1^2 - U^2)/e. \tag{40}$$

The number density of ions (or electrons) at any point is determined from the Boltzmann relation (4)

$$n_1 = n_0 \exp(eV_1/kT_e). \tag{41}$$

Now consider the pre-sheath. Differentiating ϕ_2, given by equation (32), we find the velocity components

$$v_{2r} = -\partial\phi_2/\partial r$$

$$= v_0 - C_1 R_1'(r)\cos\theta \tag{42}$$

and

$$v_{2\theta} = -\frac{1}{r}\frac{\partial\phi_2}{\partial\theta}$$

$$= C_1 r^{-1} R_1(r)\sin\theta. \tag{43}$$

v_2, V_2 and n_2 in the pre-sheath region are determined as before and are given by substituting subscript 2 for 1, in equations (39), (40) and (41). We showed in § 4 that $v_0 \to -c$ at the plasma boundary $r = a$ and we have already used the condition that $R_1' = 0$ there in deriving equation (34). Hence equation (42) gives

$$v_{2r}(a) = -c \tag{44}$$

thereby confirming Stangeby and Allen's (1970) theorem that the plasma boundary is a Mach surface.

Also, from equation (43) the tangential velocity at the plasma boundary is

$$v_{2\theta}(a) = C_1 a^{-1} R_1(a)\sin\theta \tag{45}$$

so that $v_{2\theta}$ vanishes on the axis of symmetry and is a maximum when $\theta = \frac{1}{2}\pi$.

The total ion velocity is then

$$v_2(a) = c\{1 + C_1^2 a^{-2} R_1^2(a)\sin^2\theta\}^{1/2} \tag{46}$$

which means that, in general, the ions are actually *supersonic* at the plasma boundary.

Equations (40) and (41) then give

$$V_2(a) = -\left(\frac{kT_e}{2e}\right)\{1 + C_1^2 a^{-2} R_1^2(a)\sin^2\theta - U^2\} \tag{47}$$

and

$$n_2(a) = n_0 \exp[-\tfrac{1}{2}\{1 + C_1^2 a^{-2} R_1^2(a)\sin^2\theta - U^2\}] \tag{48}$$

substituting subscript 2 for 1.

An interesting physical effect occurs on the axis of symmetry on the *downstream* side of the probe, arising from the fact that the probe actually draws ions over the whole of its surface. This is easily seen by considering equation (44); since the radial component of the ion velocity reaches sonic velocity over the entire plasma boundary, it follows that some ions reverse their direction of motion on the downstream side of the probe. Hence, there must exist a stagnation point (where the total ion velocity is zero) on the downstream side of the probe. This effect has been discussed qualitatively by Lam and Greenblatt (1965). The electrostatic potential V_0 at the stagnation point where $v = 0$ is found directly by applying energy conservation to the ions, that is,

$$V_0 = -\tfrac{1}{2}m_i U^2/e. \tag{49}$$

In principle we can choose our arbitrary separation into free stream and pre-sheath regions (i.e. we can choose the radius of the matching sphere) to make the stagnation point lie in either region. (Either v_{1r} or v_{2r}, given by equations (39) and (42), can have zeros on the axis of symmetry $\theta = 0$.) However, our choice must be consistent with our approximations. We have assumed that in the pre-sheath there is a linear perturbation to the radially symmetric ion flow. It is therefore apparent without the need for detailed numerical computation (although this could be carried out if desired) that this approximation is better when the stagnation point is taken to lie outside the pre-sheath. Furthermore, the approximation made in the free stream is that $v^2 \ll c^2$ and this is clearly particularly good around the stagnation point (where $v \to 0$) if it lies in the free stream.

Thus we take the stagnation point to be in the free stream. Its actual position is obtained by setting $\theta = v_{1r} = 0$ in equation (37); this yields a cubic equation in r_0/s

$$\left(\frac{r_0}{s}\right)^3 + \frac{v_0(s)}{U}\frac{r_0}{s} - \frac{2(1-\alpha)}{2+\alpha} = 0. \tag{50}$$

Only one root of equation (50) is both real and positive, and this gives the position of the stagnation point; solutions with $r_0/s < 1$ are not allowed. The coefficients of equation (50) are functions of s, so the calculated position of the stagnation point depends on the choice of s, the radius of the matching sphere. Figure 4 shows numerically how the solution of equation (50), r_0/a, varies with s/a for various values of the Mach number (at infinity) $M = U/c$. It can be seen that, for any given M, there is a very flat minimum in r_0/a; for convenience we choose the radius of the matching sphere s to give the minimum r_0/a. Computation of $v_1{}^2/c^2$, v_{2r}, $v_{2\theta}$ and v_0 from equations (39), (42), (43) and (9) shows that the errors in the free stream and the pre-sheath solutions are both small. Hence this choice of s is reasonable. Table 1

Table 1. Variation of the normalized position and potential at the stagnation point with Mach number

r_0/a	eV_0/kT_e	M
∞	0	0
3·534	−0·001	0·05
2·563	−0·005	0·1
1·912	−0·020	0·2
1·645	−0·045	0·3
1·498	−0·08	0·4
1·403	−0·125	0·5

gives the computed values of r_0/a, from equation (50), and eV_0/kT_e, from equation (49), for various M. The flatness of the minimum and, hence, the insensitivity of the position of the stagnation point both suggest that the particular choice of s is not very critical in obtaining an adequate approximation.

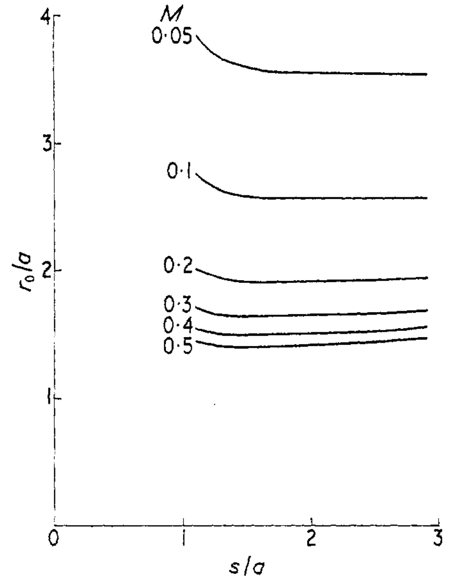

Figure 4. Variation of the position of the stagnation point with the radius of the matching sphere for various Mach numbers.

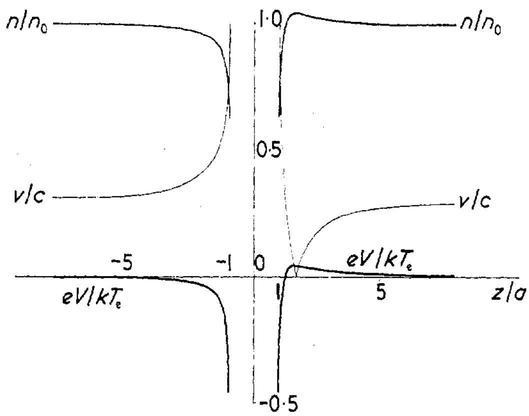

Figure 5. Normalized velocity, potential and density profiles on the axis of symmetry for $M = 0\cdot3$ (the probe occupies $-1 \leqslant z/a \leqslant 1$).

Having chosen a satisfactory radius of the matching sphere s we can now calculate the coefficients B_0, B_1 and C_1, given by equations (27), (28) and (30). Figures 1 and 2 show the ion trajectories for $M = 0\cdot1$ and $0\cdot3$, respectively, which have been obtained numerically, starting at the probe surface and using the formula

$$\theta + \arctan(v_\theta/v_r)$$

for the direction of the ion flow at any point with respect to the axis of symmetry.

v_r and v_θ are calculated numerically from equations (37), (38), (42) and (43). As would be expected from physical considerations, the stagnation point recedes from the probe as M decreases; for $M = 0$ (the radially-symmetric case) the stagnation point is at infinity and V_0 is zero. Figure 5 shows the velocity, potential and density profiles on the axis of symmetry calculated numerically from equations (39), (40) and

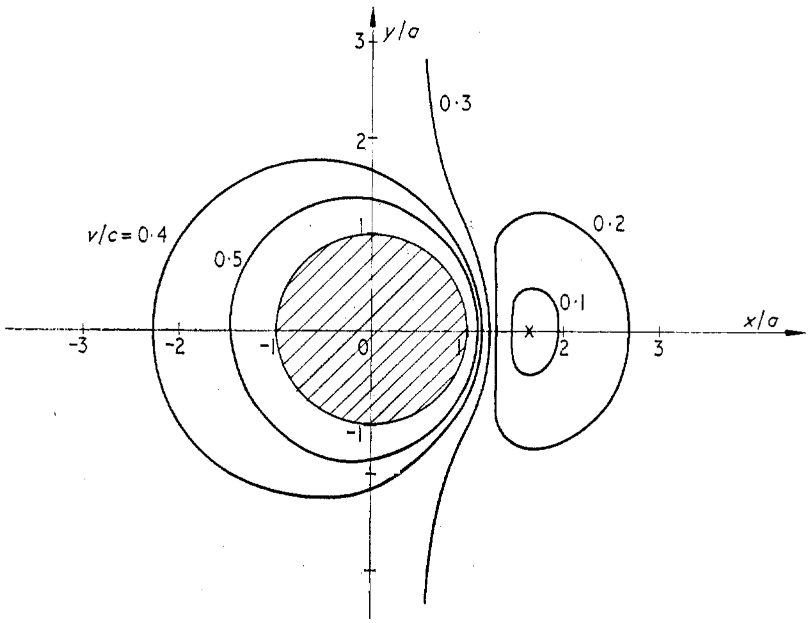

Figure 6. Contours of the normalized velocity v/c for $M = 0{\cdot}3$.

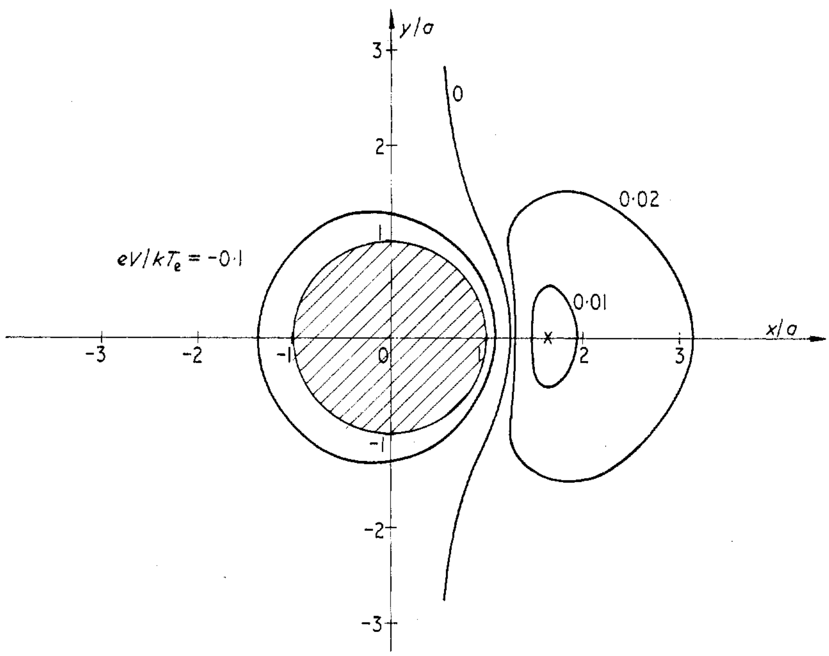

Figure 7. Contours of the normalized potential eV/kT_e for $M = 0{\cdot}3$.

(41) for $M = 0{\cdot}3$. Figures 6 and 7 are contour plots of velocity and potential, respectively, also for $M = 0{\cdot}3$. Figures 5–7 all clearly show the stagnation point on the downstream side of the probe and the breakdown of the plasma solution at the probe itself (where the velocity, potential and density gradients normal to the probe surface blow-up).

7. Saturated ion current and floating potential

The ion current to a highly negative probe in a plasma with cold ions is essentially saturated; for a given M (i.e. a given ion flow velocity at infinity) the ion current drawn by the probe is independent of the voltage V_p applied to the probe, provided the sheath thickness is small compared with the probe radius. However, the ion current collected by the probe, I_i, does depend on M and is given by

$$I_i = 2\pi a^2 e \int_0^{\pi} n_2(a) v_{2r}(a) \sin\theta \, d\theta.$$

Substituting for $n_2(a)$ and $v_{2r}(a)$ from equations (44) and (48), after some manipulation we obtain

$$I_i = 4\pi a^2 n_0 e c F(\beta) \exp\{-\tfrac{1}{2}(1-M^2+2\beta^2)\} \tag{51}$$

where

$$\beta = \frac{C_1 R_1(a)}{2^{1/2} a} \tag{52}$$

and

$$F(\beta) = \beta^{-1} \int_0^{\beta} \exp x^2 \, dx. \tag{53}$$

Typically $\beta \ll 1$, so that we can use the series

$$F(\beta) = \sum_{p=0}^{\infty} \frac{\beta^{2n}}{\{n!(2n+1)\}}. \tag{54}$$

Thus the fractional increase in ion current due to the flow velocity U (free stream Mach number M) is

$$\frac{\Delta I_i}{I_i} = \frac{I_i(M) - I_i(0)}{I_i(0)}$$

$$= F(\beta)\exp\{\tfrac{1}{2}M^2 - \beta^2\} - 1 \tag{55}$$

$$= G(M) \text{ say}. \tag{56}$$

For small M, β is $O(M)$ and

$$G(M) = \{1 + \tfrac{1}{3}\beta^2 + O(M)\}\{1 + \tfrac{1}{2}M^2 - \beta^2 + O(M^4)\} - 1$$

$$= \tfrac{1}{2}M^2 - \tfrac{2}{3}\beta^2 + O(M^4). \tag{57}$$

Figure 8 shows how $G(M)$ varies with free stream ion flow M; $G = 0$ for $M = 0$ and we recover the case of a probe collecting a radially symmetric ion flow. $G(M)$ represents a small but significant change in ion flow and so two points must be noted. The most obvious feature of this result is that $G(M)$ is still fairly small—only 5% —even when the plasma is flowing at half the speed of sound. Thus the ion current is not very greatly influenced by flow (at least when it is subsonic). The effect for low-pressures is limited to small fractional changes (rather than the two orders of magnitude found in the high-pressure case) and the existing probe analyses, which assume spherical symmetry throughout the plasma, are substantially correct numerically.

Nevertheless, the change in ion current is significant and should certainly be observable; it should be quite possible to use it to measure the ion velocity. Unfortunately the absolute values of the electron temperature and plasma density are not usually known very accurately so the absolute accuracy of the ion flow measurement (which is directly related to these quantities) would not be very great. However, the basic electron parameters (n_0, T_e) do not usually vary by more than a few per cent as we scan a plasma spatially with a probe. It should therefore be possible to measure relative differences in ion flow velocity across a plasma to within say 10%. Difficulties can however arise in determining saturated ion current since if the probe is biased sufficiently to repel most of the electrons it may influence the fields and ion flow for a fair way around the probe. It may therefore be preferable to work in terms of floating potential.

The electron current collected by the probe is given by

$$I_e = -4\pi a^2 n_0 e \left(\frac{kT_e}{2\pi m_e}\right)^{1/2} \exp\left(\frac{eV_f}{kT_e}\right) \tag{58}$$

using the Boltzmann relation (4) where m_e is now the electron mass; V_f is the probe potential. When the probe is floating the net current is zero. Equating (51) and (58) we find, with some rearrangement that

$$V_f = -\left(\frac{kT_e}{e}\right)\left[\tfrac{1}{2}\left\{1+\ln\left(\frac{m_i}{2\pi m_e}\right)\right\} - \ln\{1+G(M)\}\right]. \tag{59}$$

The fractional change in floating potential produced by the flow is therefore

$$\begin{aligned}\frac{\Delta V_f}{V_f} &= \frac{V_f(M)-V_f(0)}{V_f(0)}\\ &= -\frac{\ln\{1+G(M)\}}{\tfrac{1}{2}\{1+\ln(m_i/2\pi m_e)\}}\\ &\simeq -\frac{G(M)}{\tfrac{1}{2}\{1+\ln(m_i/2\pi m_e)\}}\\ &= -\frac{0{\cdot}30\,G(M)}{1+0{\cdot}15\ln W}\end{aligned}$$

where W is the atomic weight of the ion species, m_i/m_H. Now $\tfrac{1}{2}\{1+\ln(m_i/2\pi m_e)\}$ is eV_f/kT_e for the no-flow case. It is the floating probe potential (with no flow) compared with the electron temperature (in volts). It varies from plasma to plasma, from 3·34 for atomic hydrogen to 5·99 for mercury, like $\{1+0{\cdot}15\ln W\}^{-1}$, or a factor of nearly two over the whole periodic table.

It may be noted that the fractional reduction in saturation ion current is the same for all gases (at a given flow velocity), although the absolute value of the current does of course vary from gas to gas (like $m_i^{-1/2}$). Thus the change in floating potential is less than half that in ion saturation current. However, since a floating probe will disturb the plasma less than one biased sufficiently to collect only ion current, this

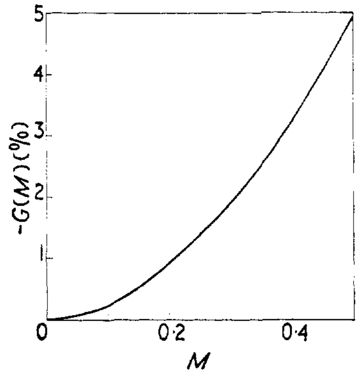

Figure 8. Variation of $G(M)$ with Mach number (at infinity) M.

measurement may be preferable. Floating potentials are usually repeatable to within a per cent or so, and so differences in ion flow velocity throughout a plasma should be measurable to within a few per cent.

8. Conclusions

A selfconsistent model can be obtained for subsonic ion flow past a negative spherical probe immersed in a collisionless ionization-free plasma. A stagnation point arises on the downstream side of the probe which clearly cannot exist in a symmetrical, static situation. Although the saturation ion current and the floating potential given by previous analyses (which all assume spherical symmetry) are substantially correct, there is some dependence on the ion flow velocity (a few $^0/_0$ at $M = 0{\cdot}5$). Thus the change in floating potential can be used to measure ion flow. Apart from this, only slight modifications need to be made to low pressure probe theories in order to include flow effects.

Acknowledgments

This work was carried out at Marchwood Engineering Laboratories and is published with the permission of the Central Electricity Generating Board.

References

Allen, J. E., and Andrews, J. G., 1970, *J. Plasma Phys.*, **4**, 187.

Allen, J. E., Boyd, R. L. F., and Reynolds, P., 1957, *Proc. Phys. Soc.* B, **70**, 297.

Andrews, J. G., 1970, *Phys. Fluids*, to be published.

Andrews, J. G., and Stangeby, P. C., 1970, *J. Phys.* A: *Gen. Phys.*, **3**, L39–40.

Bernstein, I. B., and Rabinowitz, I., 1959, *Phys. Fluids*, **2**, 112

Bertotti, B., Cavaliere, A., and Giupponi, P., 1966, *Phys. Fluids*, **9**, 265.

Bienkowski, G. K., and Chang, K. W., 1968, *Phys. Fluids*, **11**, 784.

Bohm, D., Burhop, E. H. S., and Massey, H. S. W., 1949, *The Characteristics of Electrical Discharges in Magnetic Fields*, Eds A. Guthrie and R. K. Wakerling (New York: McGraw Hill), chap. 2.

Clements, R. M., and Smy, P. R., 1969, *J. Phys.* D: *Appl. Phys.*, **2**, 1731. (See also 1970, *J. appl. Phys.*, **41**, 3745, for the cylindrical case.)

FORREST, J. R., and FRANKLIN, R. N. 1966, *Br. J. appl. Phys.*, **17,** 1061.
—— 1968, *J. Phys.* D: *Appl. Phys.*, **1,** 1357.
LAM, S. H., 1965, *Phys. Fluids*, **8,** 73.
LAM, S. H., and GREENBLATT, M., 1965, *Proc. 4th Int. Symp. on Rarefied Gas Dynamics*, Ed. J. H. de Leeuw (New York: Academic), 45.
MOTT-SMITH, H., and LANGMUIR, I., 1926, *Phys. Rev.*, **28,** 727.
ROSA, R., and ALLEN, J. E., 1970, *J. Plasma Phys.*, **4,** 195.
SNEDDON, I. N., 1956, *Special Functions of Mathematical Physics and Chemistry* (Edinburgh: Oliver and Boyd), chap. 3.
STANGEBY, P. C., and ALLEN, J. E., 1970, *J. Phys.* A: *Gen. Phys.*, **3,** 304.
SU, C. H., and LAM, S. H., 1963, *Phys. Fluids*, **6,** 1479.
THOMAS, D. L., 1969, *Electron. Lett.*, **5,** 341.
WOODS, L. C., 1965, *J. Fluid Mech.*, **23,** 315.